INORGANIC CHEMISTRY FRONTIERS

RESEARCH ARTICLE

View Article Online
View Journal | View Issue

Cite this: *Inorg. Chem. Front.*, 2026, **13**, 1515

Isocyanide insertion reaction of a carborane-fused borirane and isocyanide affinity of the ring expansion products

Libo Xiang,[a] Junyi Wang,[b] Julius Bolch,[a] Alexander Matler[a] and Qing Ye *[a]

Received 29th October 2025,
Accepted 5th December 2025

DOI: 10.1039/d5qi02191j

rsc.li/frontiers-inorganic

The reactions of the carborane-fused borirane $(B_{10}H_{10}C_2)BN(SiMe_3)_2$ (**1**) with isocyanides proceed, for the first time, with a clearly defined sequence of coordination and insertion steps. The first equivalent of isocyanide undergoes selective 1,1-insertion into the borirane unit, affording a four-membered borete ring (**2**). A second equivalent initially coordinates reversibly to the boron center. Subsequent heating promotes its full insertion to generate the α-diimine product (**3**), which can reversibly capture an additional isocyanide molecule. Variable-temperature NMR studies reveal that **3** exhibits a remarkably higher isocyanide affinity than **2**.

Introduction

Boriranes[1] (**I** in Fig. 1) are a class of three-membered boron heterocycles composed of a tricoordinate boron center and two saturated carbon atoms. In contrast to their unsaturated counterparts, *i.e.* borirenes, boriranes lack aromatic stabilization. Therefore, boriranes exhibit higher ring strain energy and Lewis acidity. The most reported boriranes are synthesized as Lewis base adducts (**II**), representing a class of boron-isosteres of cyclopropanes.[2] However, in sharp contrast to cyclopropanes, the reactivity of boriranes has remained largely underexplored.

In recent years, increasing ring strain *via* annulation has emerged as a strategy to unlock the reaction chemistry of boriranes. A notable example is the fusion of a borirane ring with an *o*-carborane cage through a shared carbon–carbon bond (**III**).[3] In addition to boosted ring strain energy, the *o*-carborane-fused boriranes exhibit boosted Lewis acidity due to the strong electron withdrawing nature of the *o*-carborane framework.[4] This enables a stronger interaction between the boron center of the borirane and Lewis bases (**IV**), which in turn promotes ring-opening,[1,5] rearrangement,[6] and particularly ring enlargement reactions.[3b,5] The difference in the reactivity of the *o*-carborane-fused aminoborirane **1** (Scheme 1) and its benzo-fused counterpart toward THF clearly highlights the impact of *o*-carborane fusing on the reactivity.[3a,6] While **1** readily coordinates to THF and subsequently undergoes a ring-opening rearrangement to afford the first free carboranyl iminoborane, its benzo-fused counterpart is not Lewis acidic enough to bind THF, thereby preventing further reactions.[6]

The ring enlargement reactions reported for carborane-fused boriranes include: insertion of a sulfur atom into the B–C_{Cb} bond of a carbene-stabilized borirane;[5a] σ-bond insertion, for example, treatment of a carborane-fused borirane with BBr_3, $GeCl_2$ or $GaCl_3$ leads to the insertion of the E–X σ-bond into the strained ring, with the E–X bond being converted into a dative interaction; 1,2-insertion of unsaturated polar bonds, a reaction mode that has demonstrated broad substrate scope, including alkyl ketones,[5] aldehydes,[3b,5b] nitriles,[3b,c,5b] CO_2,[5b] as well as Bestmann ylide;[7] and 1,4-insertion of benzophenone, which involves dearomatization of one of the phenyl rings.[3b]

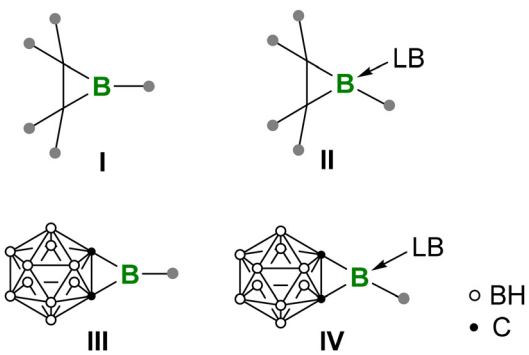

Fig. 1 Boriranes (I), carborane-fused boriranes (III), and their Lewis base (LB) adducts (II and IV).

[a]*Institute for Inorganic Chemistry and Institute for Sustainable Chemistry & Catalysis with Boron, Julius-Maximilians-Universität Würzburg, Am Hubland, 97074 Würzburg, Germany. E-mail: qing.ye@uni-wuerzburg.de*
[b]*Department of Chemistry and Biochemistry, Baylor University, Waco, Texas 76798, USA*

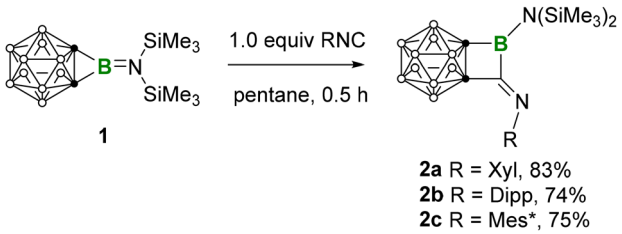

Scheme 1 Reaction of **1** with 1.0 equiv. RNC (R: Xyl = 2,6-MeC_6H_4; Dipp = 2,6-$iPr_2C_6H_4$; Mes* = 2,4,6-$tBu_3C_6H_2$).

Indeed, the high versatility of the ring enlargement reactions highlights the potential of carborane-fused boriranes as modular building blocks for constructing novel carborane-based functional molecules.[8] Isocyanides exhibit rich reactivity.[9] In particular, their insertion chemistry makes them valuable C1 synthons and offers great potential in skeletal editing.[10,11] However, the reactivity between boriranes and isocyanides has not been reported thus far.

Herein, we exploit a carborane-fused borirane of type **III**, which features both boosted ring strain energy from annulation and a non-coordinated boron center, to realize for the first time the reaction of borirane with isocyanides, enabling the modular construction of carborane-fused boretes and borirane-derived α-diimines.

Results and discussion

o-Carborane-fused aminoborirane **1** underwent a rapid and selective reaction with 1.0 equivalent of RNC (R = Dipp, Xyl or Mes*) in pentane at room temperature (Scheme 1), leading to the quantitative formation of a new boron-containing species **2** (**2a**, δ_B 41.9; **2b**, δ_B 42.5, and **2c**, δ_B 42.8). Single crystals of **2** were obtained by storing the reaction mixtures at −30 °C in a glovebox refrigerator over a period of 12 hours. Single crystal X-ray diffraction analysis of **2a–c** revealed the *o*-carborane-fused borete structures as depicted in Fig. 2, with one isocyanide unit being 1,1-inserted. The exohedral boron within the borete unit adopts a distorted trigonal planar geometry with a surrounded angle sum of 360° (**2a**, 360.0°; **2b**, 360.0°; and **2c**, 359.8°) and an acute internal angle (**2a**, 88.98(9)°; **2b**, 89.18 (17)°; and **2c**, 89.4(2)°). Besides, the dihedral angles C1–B1–C2–C3 of **2a** (−4.668°), **2b** (1.517°) and **2c** (−2.032°) reflect the planar geometry of the borete ring. The exocyclic C1–N1 lengths of 1.2599(16) Å (**2a**), 1.261(3) Å (**2b**) and 1.266(4) Å (**2c**) fall within the range of typical C–N double bond distances. It should be noted that although isocyanide insertion reactions also occur in benzo-fused analogues (*i.e.* benzoborirenes[12]), the mono-insertion products are difficult to isolate or even to observe.[12b] To date, the only reported example of a mono-insertion product was achieved using the very bulky Mes*NC.[12a]

Interestingly, even the addition of one more equivalent of the corresponding isocyanide to **2a** or **2b** at room temperature does not result in a second insertion. Instead, the isocyanide coordinates to the boron center of **2a**/**b** to afford adduct **3a**/**b**. However, since this coordination is rather weak, a dissociation equilibrium is present in solution at room temperature

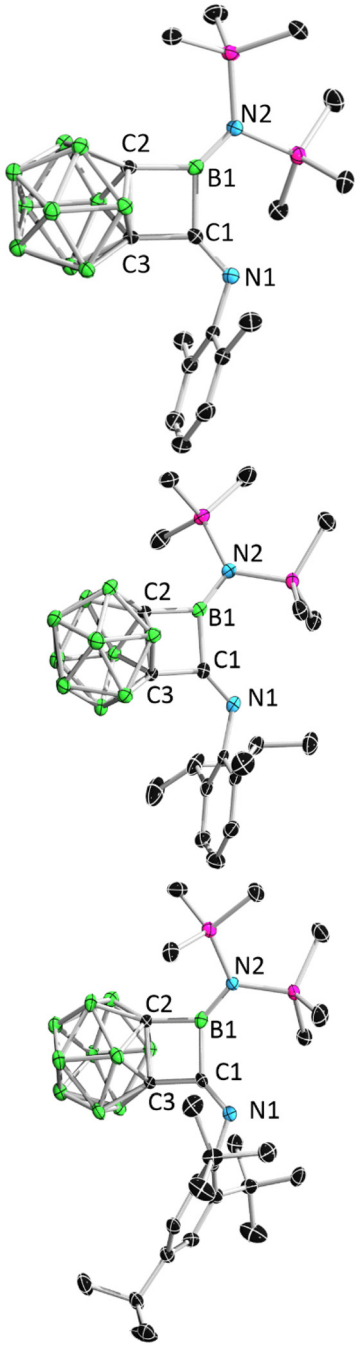

Fig. 2 Single crystal structure of **2a** (upper), **2b** (middle) and **2c** (bottom). Hydrogen atoms have been removed for clarity. Thermal ellipsoids are drawn at the 50% probability level. Selected bond lengths [Å] and angles [°]: **2a**, B1–C1 1.6341(18), B1–C2 1.6469(18), B1–N2 1.3827 (17), C1–N1 1.2599(16), C1–B1–C2 88.98(9); **2b**, B1–C1 1.636(3), B1–C2 1.642(3), B1–N2 1.379(3), C1–N1 1.261(3), C1–B1–C2 89.18(17); **2c**, B1–C1 1.640(5), B1–C2 1.642(4), B1–N2 1.385(4), C1–N1 1.266(4), C1–B1–C2 89.4(2).

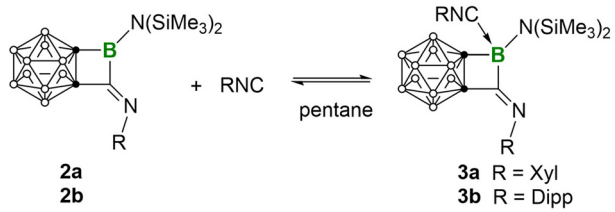

Scheme 2 Equilibrium between **2a/b** and **3a/b** in pentane.

(Scheme 2), as evidenced by the only slight upfield shift of the ^{11}B NMR signals: **2a** δ_B 41.9 → 36.3, **2b**, δ_B 42.5 → 36.6. Moreover, storing the pentane solution at −30 °C for 2 hours affords single crystals of **3a**/**b** suitable for X-ray diffraction analysis. Redissolving these crystals in pentane affords a solution displaying the same NMR signals as the aforementioned reaction mixture. In the solid-state structure, the second isocyanide unambiguously coordinates to the B1 center, with a B1–C4 distance (**3a**: 1.6437(16) Å and **3b**: 1.656(2) Å) expected for a C → B dative bond (Fig. 3). In addition, the increased coordination number at B1 leads to elongation of the surrounding bonds. In contrast, treatment of **2c** with 1.0 equivalent of Mes*NC does not cause any change in the ^{11}B NMR spectrum. It is nevertheless not surprising that **2c** cannot further react with Mes*NC due to the steric hindrance.

On the NMR timescale, a rapid dynamic equilibrium process results in an averaged chemical shift that reflects the distribution of the species in equilibrium. Therefore, to gain further insight into the dissociation equilibrium of isocyanide, variable-temperature NMR (VT-NMR) experiments were conducted on **3a**. As depicted in Fig. 4, as the temperature decreased, the ^{11}B NMR signal of atom B1 gradually shifted upfield until it was obscured by the high-field resonances of the carborane cage. This observation is consistent with the expected enthalpy-driven formation of the adduct at lower temperatures. To further estimate the thermodynamic parameters of this equilibrium, the ^{11}B-NMR signal of atom B1 in **2a** (δ_B 41.9) as well as that in **3a** was required. However, since the B1 signal of **3a** overlapped with the signals of the carborane cage, its value (δ_B −4.3) could only be obtained through theoretical calculations at the M06L/pcSseg-2//PBEh-3c/def2-mSVP level of theory. To verify the reliability of this computational approach, the ^{11}B-NMR signal of **2a** was calculated using the same method, which showed excellent agreement with the experimental value (theo. δ_B: 40.2 *vs.* exp. δ_B: 41.9). Based on the ^{11}B-NMR signals of atom B1 in **2a** (δ_B 41.9) and **3a** (δ_B −4.3), fitting of the variable temperature data to the Van't Hoff equation affords the enthalpy (ΔH° = −38.0 ± 0.8 kJ mol^{-1}) and entropy (ΔS° = −146.1 ± 3.2 J mol^{-1} K^{-1}) (R^2 = 0.99). See the SI for details. From these values, the Gibbs free energy at 298 K was estimated to be ΔG° = 5.5 kJ mol^{-1}.

Furthermore, **3a** and **3b** were found to undergo a slow transformation at room temperature, requiring about 8 days to form a new three-coordinate boron-containing species showing a ^{11}B-NMR resonance at δ_B 46.7 (**3a′**) and δ_B 45.5 (**3b′**),

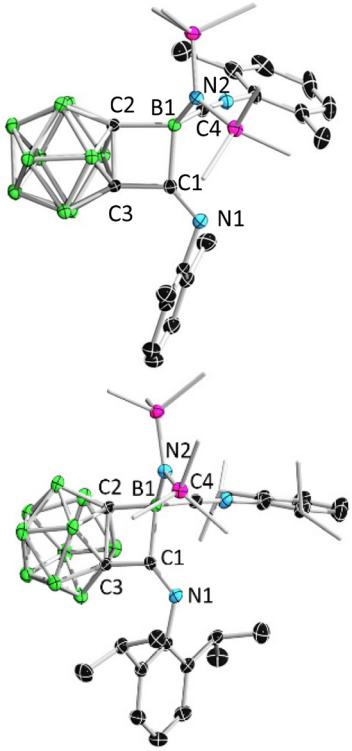

Fig. 3 Single crystal structure of **3a** (upper) and **3b** (bottom). Hydrogen atoms have been removed for clarity. Thermal ellipsoids are drawn at the 50% probability level. Selected bond lengths [Å] and angles [°]: **3a**, B1–C1 1.6913(17), B1–C2 1.7000(16), B1–C4 1.6437(16), B1–N2 1.4957(16), C1–N1 1.2630(15), C1–B1–C2 85.11(8); **3b**, B1–C1 1.688(2), B1–C2 1.711(2), B1–C4 1.656(2), B1–N2 1.496(2), C1–N1 1.2609(18), C1–B1–C2 84.79(10).

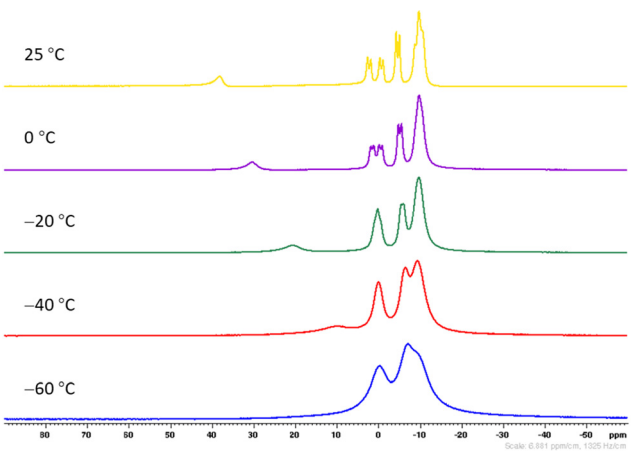

Fig. 4 ^{11}B NMR (192 MHz, toluene-d_8) spectra of **3a** at various temperatures.

respectively, accompanied by a distinct color change from yellow to reddish-brown. Heating the sample to 80 °C significantly accelerated this process, affording the same product within only 4 hours. In contrast to **3a**/**b**, in which the isocya-

nide coordinated to boron readily dissociates so that only the molecular signals of **2a**/**b** can be detected by high-resolution mass spectrometry (HRMS), the spectra of **3a′**/**3b′** clearly display molecular signals corresponding to **2a**/**b** with an extra equivalent of the respective isocyanide. This suggests that the second isocyanide becomes firmly incorporated through insertion (Scheme 3). However, all attempts to grow single crystals of **3a′**/**3b′** were unsuccessful. Therefore, we decided to further convert them into Lewis base adducts, which facilitate crystallization. To this end, **3a′**/**3b′** was further treated with one more equivalent of the respective isocyanide at room temperature. The tricoordinate boron signal disappeared rapidly, indicating that the isocyanide indeed coordinated to the tricoordinate boron center, affording **4a**/**b** (Scheme 3). This was further confirmed by single crystal characterization (Fig. 5).

In sharp contrast to **2a**/**b**, which mainly exist in a non-coordinated form in the presence of one equivalent of isocyanide at room temperature, **3a′**/**3b′** readily form adducts under the same conditions, with the equilibrium (Scheme 4) shifting gradually toward dissociation of the adducts upon heating. As shown in Fig. 6, VT-NMR data of **4a** show that upon increasing the temperature, the signal corresponding to the three-coordinate boron species appears and gradually shifts downfield, reaching 45.7 ppm at 100 °C. This value is nearly identical to that of **3a′** (46.7 ppm), indicating that **4a** exists predominantly in the non-coordinated form in solution at 100 °C. To quantify the thermodynamic parameters of this equilibrium, the ^{11}B resonance of the four-coordinate species in **4a** was obtained by DFT calculations (δ_B −8.2), since this signal is obscured within the resonance region of the carborane cage and thus difficult to identify experimentally. To ensure the reliability of the calculated NMR shifts, we also computed the ^{11}B chemical shift of **3a′**, which showed agreement with the experimental value (theo. δ_B 41.5 *vs.* exp. δ_B 46.7). Van't Hoff fitting of the data gave the enthalpy ($\Delta H° = -45.1 \pm 2.9$ kJ mol^{-1}) and entropy ($\Delta S° = -153.1 \pm 8.3$ J mol^{-1} K^{-1}) ($R^2 = 0.98$). At 298 K, the corresponding Gibbs free energy is $\Delta G° = 0.5$ kJ mol^{-1}. See the SI for details. Remarkably, **3a′** exhibits higher isocyanide affinity than **2a** (**3a′**: −45.1 ± 2.9 kJ mol^{-1} *vs.* **2a**: −38.0 ± 0.8 kJ mol^{-1}). This may be attributed to the presence of additional electron-withdrawing imino groups near the three-coordinate boron center in **3a′**. Furthermore, likely due to steric hindrance, further heating of **4a**/**b** did not promote insertion of the third equivalent of isocyanide. No detectable spectral changes occurred even after prolonged heating at 110 °C in toluene-d_8 for one week.

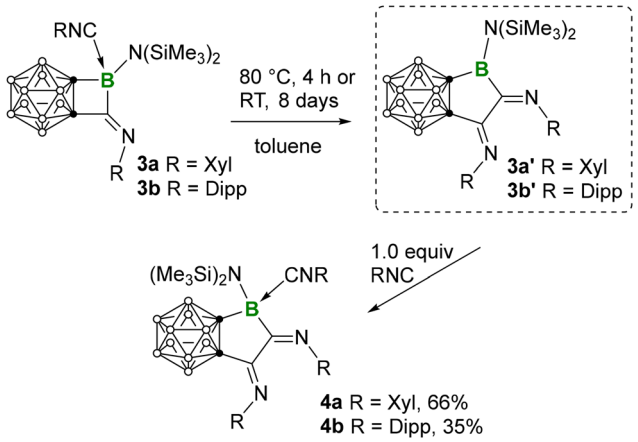

Scheme 3 Synthesis of **4a**/**b** *via* **3a′**/**3b′**.

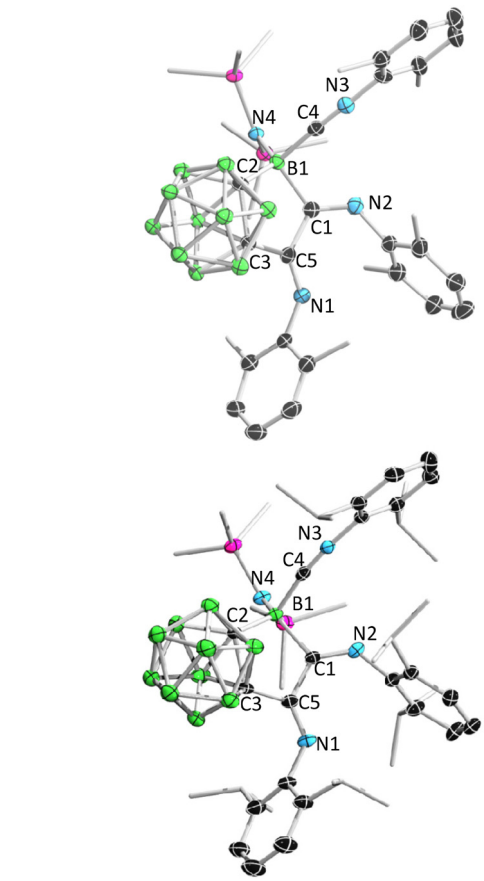

Fig. 5 Single crystal structure of **4a** (upper) and **4b** (bottom). Hydrogen atoms have been removed for clarity. Thermal ellipsoids are drawn at the 50% probability level. Selected bond lengths [Å] and angles [°]: **4a**, B1–C1 1.673(2), B1–C2 1.665(2), B1–C4 1.634(2), B1–N4 1.5178(19), C1–N2 1.281(2), C5–N1 1.263(2), C5–C1 1.517(2), C1–B1–C2 99.65(11); **4b**, B1–C1 1.676(4), B1–C2 1.671(5), B1–C4 1.644(5), B1–N4 1.515(4), C1–N2 1.277(4), C5–N1 1.265(4), C5–C1 1.526(4), C1–B1–C2 98.8(2).

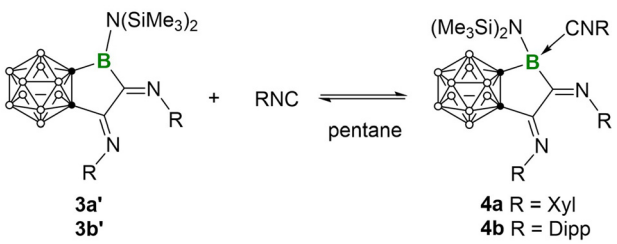

Scheme 4 Equilibrium between **3a′**/**3b′** and **4a**/**b** in pentane.

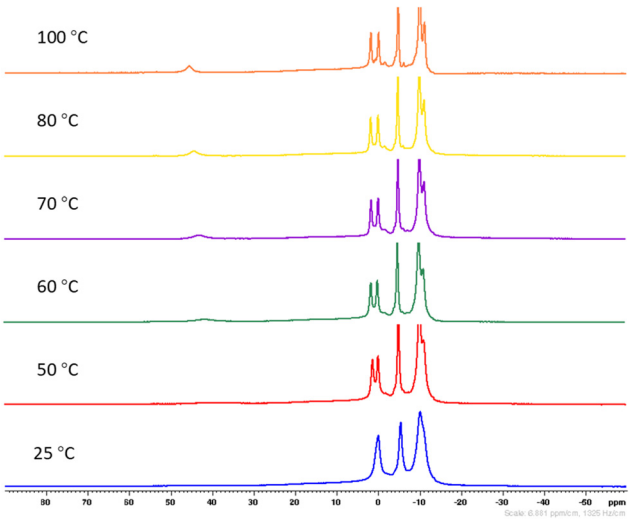

Fig. 6 ^{11}B NMR (192 MHz, toluene-d_8) spectra of **4a** at various temperatures.

Conclusion

In summary, we have for the first time realized the isocyanide insertion reaction of a carborane-fused borirane derivative, further demonstrating the potential of boriranes as versatile BC_2 synthons. This type of transformation offers a new strategy for constructing next-generation bora-heterocyclic compounds. Moreover, detailed NMR experiments, isolation and characterization of intermediates allowed the reaction sequence to be clearly elucidated. This provides a general picture of isocyanide promoted ring expansion reactions of boracycles. The double-insertion product exhibits a significantly higher isocyanide affinity than the mono-insertion product, reflecting the non-negligible electron-withdrawing effect of the imino substituents in enhancing the Lewis acidity of the boron center.

Experimental section

General procedures

All manipulations were conducted under an atmosphere of dry argon, using either a standard Schlenk line or a glovebox. Solvents were purified by distillation from Na/K under dry argon. C_6D_6 was degassed by three freeze–pump–thaw cycles and stored over molecular sieves. Borirane **1** was prepared according to a published procedure.[3a] NMR spectra were acquired on a Bruker Avance 400 (^{1}H: 400.1 MHz, ^{11}B: 128.4 MHz, ^{13}C: 100.6 MHz) NMR spectrometer at 298 K. Variable-temperature NMR experiments were performed on a Bruker Avance III 600 spectrometer (^{1}H: 600 MHz, ^{11}B: 192 MHz). ^{1}H, ^{13}C{^{1}H} and ^{1}H{^{11}B} spectra were referenced to external TMS. ^{11}B and ^{11}B{^{1}H} NMR spectra were referenced to external $BF_3{\cdot}OEt_2$. High resolution mass spectrometry (HRMS) was performed with a Thermo Fisher Scientific Q-Exactive MS System. Elemental analysis (C, H, and N) was performed on a Vario MICRO Cube CHNS analyzer.

Synthesis of 2

RNC (1 eq., 0.25 mmol) was added to borirane **1** (80 mg, 0.25 mmol) in 1 mL pentane at room temperature. After stirring for 0.5 h at room temperature, the reaction system was cooled to −30 °C for 12 h. The crystals were separated from the mother liquid by filtration, washed with cold pentane, and dried under vacuum to give analytically pure **2**.

2a (light green block crystals, 96 mg, 83%): **^{1}H NMR** (C_6D_6): δ = 6.90 to 6.84 (m, 3H, C*H* of Xyl), 3.64 to 2.18 (m, 10H, B*H*), 2.01 (s, 6H, C*Me*$_3$), 0.23 (s, 18H, Si*Me*$_3$); **^{1}H{^{11}B} NMR** (C_6D_6): δ = 6.91 to 6.85 (m, 3H, C*H* of Xyl), 3.04 (s, 1H, B*H*), 3.00 (s, 1H, B*H*), 2.88 (s, 2H, B*H*), 2.75 (s, 2H, B*H*), 2.58 (s, 2H, B*H*), 2.20 (s, 2H, B*H*), 2.01 (s, 6H, C*Me*$_3$), 0.23 (s, 18H, Si*Me*$_3$); **^{11}B NMR** (C_6D_6): δ = 41.9 (s, *B*N(SiMe$_3$)$_2$), 2.5 (d, J = 152.3 Hz, B_{Cb}), −0.9 (d, J = 150.1 Hz, B_{Cb}), −4.5 (d, J = 150.1 Hz, B_{Cb}), −8.6 to −11.1 (m, B_{Cb}); **^{11}B{^{1}H} NMR** (C_6D_6): δ = 42.0 (s, *B*N(SiMe$_3$)$_2$), 2.5 (s, B_{Cb}), −1.0 (s, B_{Cb}), −4.5 (s, B_{Cb}), −9.2 (s, B_{Cb}), −10.6 (s, B_{Cb}); **^{13}C{^{1}H} NMR** (C_6D_6): δ = 146.0 (*C* of Xyl), 125.1 (*C* of Xyl), 124.8 (*C* of Xyl), 89.1 (C of Cb), 18.3 (C*Me*$_3$), 3.4 (Si*Me*$_3$); **HRMS (*m*/*z*)**: [M + H_2O] calcd for $C_{17}H_{39}N_2B_{11}Si_2O$, 464.3625; found 464.3616.

2b (light green block crystals, 93 mg, 74%): **^{1}H NMR** (C_6D_6): δ = 7.07 (m, 3H, C*H* of Dipp), 2.76 (sep, J = 6.8 Hz, 2H, C*H* of *i*Pr), 1.31 (d, J = 6.9 Hz, 6H, *Me* of *i*Pr), 1.11 (d, J = 6.7 Hz, 6H, *Me* of *i*Pr), 0.25 (s, 18H, Si*Me*$_3$); **^{1}H{^{11}B} NMR** (C_6D_6): δ = 7.07 (m, 3H, C*H* of Dipp), 3.03 (s, 1H, B*H*), 2.99 (s, 1H, B*H*), 2.87 (s, 2H, B*H*), 2.76 (s, 2H, B*H*), 2.76 (sep, J = 6.8 Hz, 2H, C*H* of *i*Pr), 2.65 (s, 2H, B*H*), 2.19 (s, 2H, B*H*), 1.31 (d, J = 6.9 Hz, 6H, *Me* of *i*Pr), 1.10 (d, J = 6.8 Hz, 6H, *Me* of *i*Pr), 0.25 (s, 18H, Si*Me*$_3$); **^{11}B NMR** (C_6D_6): δ = 42.5 (s, *B*N(SiMe$_3$)$_2$), 2.1 (d, J = 143.2 Hz, B_{Cb}), 0.7 (d, J = 149.7 Hz, B_{Cb}), −4.5 (d, J = 147.3 Hz, B_{Cb}), −9.8 (m, B_{Cb}); **^{11}B{^{1}H} NMR** (C_6D_6): δ = 42.4 (s, *B*N(SiMe$_3$)$_2$), 2.6 (s, B_{Cb}), −0.8 (s, B_{Cb}), −4.5 (s, B_{Cb}), −9.3 (s, B_{Cb}), −10.4 (s, B_{Cb}); **^{13}C{^{1}H} NMR** (C_6D_6): δ = 144.0 (*C* of Dipp), 135.8 (*C* of Dipp), 125.9 (*C* of Dipp), 122.9 (*C* of Dipp), 89.6 (C of Cb), 29.0 (*C*HMe$_2$), 25.2 (CH*Me*$_2$), 21.1 (*CHMe*$_2$), 3.6 (Si*Me*$_3$); **HRMS (*m*/*z*)**: [M + H]$^+$ calcd for $C_{21}H_{46}N_2B_{11}Si_2$, 503.4223; found 503.4227; **elemental analysis**: calcd for $C_{21}H_{45}B_{11}N_2Si_2$: C, 50.38; H, 9.06; N, 5.60; found C, 50.28; H, 9.04; N, 5.47.

2c (yellow block crystals, 110 mg, 75%): **^{1}H NMR** (C_6D_6): δ = 7.35 (s, 2H, C*H* of Mes*), 3.54 to 2.24 (m, 10H, B*H*), 1.43 (s, 18H, C*Me*$_3$), 1.32 (s, 9H, C*Me*$_3$), 0.26 (s, 18H, Si*Me*$_3$); **^{1}H{^{11}B} NMR** (C_6D_6): δ = 7.35 (s, 2H, C*H* of Mes*), 3.06 (m, 2H, B*H*), 2.90 (s, 2H, B*H*), 2.79 (s, 1H, B*H*), 2.74 (s, 1H, B*H*), 2.14 (s, 2H, B*H*), 1.43 (s, 18H, C*Me*$_3$), 1.32 (s, 9H, C*Me*$_3$), 0.26 (s, 18H, Si*Me*$_3$); **^{11}B NMR** (C_6D_6): δ = 42.8 (s, *B*N(SiMe$_3$)$_2$), 2.4 (d, J = 136.6 Hz, B_{Cb}), −0.7 (d, J = 136.2 Hz, B_{Cb}), −4.4 (d, J = 138.7 Hz, B_{Cb}), −10.3 (m, B_{Cb}); **^{11}B{^{1}H} NMR** (C_6D_6): δ = 43.3 (s, Cb*B*N$_4$), 2.5 (s, B_{Cb}), −0.4 (s, B_{Cb}), −4.4 (s, B_{Cb}), −9.7 (s, B_{Cb}); **^{13}C{^{1}H} NMR** (C_6D_6): δ = 146.3 (*C* of Mes*), 144.6 (*C* of Mes*), 138.3 (*C* of Mes*), 122.4 (*C* of Mes*), 90.8 (C of Cb), 37.1 (*C*Me$_3$), 34.7 (*C*Me$_3$), 32.8 (C*Me*$_3$), 31.7 (C*Me*$_3$), 3.9 (Si*Me*$_3$); **HRMS (*m*/*z*)**: [M + OH]$^-$ calcd for $C_{27}H_{58}ON_2B_{11}Si_2$, 603.5111;

found 603.5154; **elemental analysis**: calcd for $C_{27}H_{57}B_{11}N_2Si_2$: C, 55.45; H, 9.82; N, 4.79; found C, 55.03; H, 9.96; N, 4.88.

Synthesis of 3

RNC (0.32 mmol, 2 eq.) was added to borirane **1** (50 mg, 0.16 mmol, 1 eq.) in 1 mL pentane at room temperature. Then the reaction system was quickly cooled to −30 °C for 2 h. The crystals were separated from the mother liquid and dried as an analytically pure product of **3a** or **3b**. **3a** and **3b** can also be obtained through the reaction of **2a** or **2b** and 1 eq. of RNC in pentane.

3a (colorless needle crystals, 97 mg, 88%), **^{1}H NMR** (C_6D_6): δ = 6.91 to 6.84 (m, 3H, C*H* of Xyl), 6.71 (t, J = 7.8 Hz, 1H, C*H* of Xyl), 6.55 (d, 2H, J = 7.6 Hz, C*H* of Xyl), 3.67 to 2.16 (m, 10H, B*H*), 3.06 (s, 6H, *Me* of Xyl), 2.02 (s, 6H, *Me* of Xyl), 0.26 (s, 18H, Si*Me*$_3$); **^{1}H{^{11}B} NMR** (C_6D_6): δ = 6.91 to 6.85 (m, 3H, C*H* of Xyl), 6.74 to 6.70 (m, 1H, C*H* of Xyl), 6.57 (d, J = 7.6 Hz, 2H, C*H* of Xyl), 3.04 (s, 1H, B*H*), 2.97 (s, 1H, B*H*), 2.87 (s, 2H, B*H*), 2.76 (s, 2H, B*H*), 2.64 (s, 2H, B*H*), 2.21 (s, 2H, B*H*), 2.07 (s, 6H, *Me* of Xyl), 2.03 (s, 6H, *Me* of Xyl), 0.27 (s, 18H, Si*Me*$_3$); **^{11}B NMR** (C_6D_6): δ = 36.3 (s, *B*N(SiMe$_3$)$_2$), 2.0 (d, J = 138.1 Hz, B_{Cb}), 0.8 (d, J = 146.2 Hz, B_{Cb}), −4.9 (d, J = 148.2 Hz, B_{Cb}), −8.9 (m, B_{Cb}); **^{11}B{^{1}H} NMR** (C_6D_6): δ = 36.5 (s, *B*N(SiMe$_3$)$_2$), 2.0 (s, B_{Cb}), −0.8 (s, B_{Cb}), −4.8 (s, B_{Cb}), −10.3 (s, B_{Cb}); **^{13}C{^{1}H} NMR** (C_6D_6): δ = 146.1 (*C* of Xyl), 135.0 (*C* of Xyl), 125.2 (*C* of Xyl), 124.7 (*C* of Xyl), 124.1 (*C* of Xyl), 122.8 (*C* of Xyl), 89.1 (C of Cb), 18.3 (*C*HMe$_2$), 18.2 (*C*HMe$_2$), 3.5 (Si*Me*$_3$); **HRMS (*m*/*z*)**: only **2a** was detected. **Elemental analysis**: calcd for $C_{26}H_{46}B_{11}N_3Si_2$: C, 54.24; H, 8.05; N, 7.30; found C, 53.95; H, 8.14; N, 7.12.

3a′ (brown oil): **^{1}H NMR** (C_6D_6): δ = 6.88 to 6.81 (m, 3H, C*H* of Xyl), 6.75 to 6.67 (m, 3H, C*H* of Xyl), 3.45 to 2.76 (m, 10H, B*H*), 2.02 (s, 6H, *Me* of Xyl), 1.74 (s, 6H, *Me* of Xyl), 0.31 (s, 18H, Si*Me*$_3$); **^{1}H{^{11}B} NMR** (C_6D_6): δ = 6.87 to 6.81 (m, 3H, C*H* of Xyl), 6.75 to 6.67 (m, 3H, C*H* of Xyl), 3.06 (s, 2H, B*H*), 2.86 (s, 2H, B*H*), 2.74 (s, 2H, B*H*), 2.63 (s, 2H, B*H*), 2.25 (s, 2H, B*H*), 2.03 (s, 6H, *Me* of Xyl), 1.74 (s, 6H, *Me* of Xyl), 0.31 (s, 18H, Si*Me*$_3$); **^{11}B NMR** (C_6D_6): δ = 46.7 (s, *B*N(SiMe$_3$)$_2$), 1.93 to −0.69 (m, B_{Cb}), −5.0 (d, J = 138.7 Hz, B_{Cb}), −10.8 (m, B_{Cb}); **^{11}B{^{1}H} NMR** (C_6D_6): δ = 46.6 (s, *B*N(SiMe$_3$)$_2$), 1.4 (s, B_{Cb}), −0.4 (s, B_{Cb}), −5.0 (s, B_{Cb}), −10.6 (s, B_{Cb}); **^{13}C{^{1}H} NMR** (C_6D_6): δ = 151.4 (*C* of Xyl), 144.1 (*C* of Xyl), 127.7 (*C* of Xyl), 124.5 (*C* of Xyl), 123.8 (*C* of Xyl), 123.4 (*C* of Xyl), 77.8 (C of Cb), 19.1 (*C*HMe$_2$), 18.0 (*C*HMe$_2$), 4.3 (Si*Me*$_3$); **HRMS (LIFDI)**: calcd for $C_{26}H_{46}B_{11}N_3Si_2$, 577.4254; found 577.4248.

3b (off-white block crystals, 93 mg, 74%): **^{1}H NMR** (C_6D_6): δ = 7.08 to 7.04 (m, 3H, C*H* of Dipp), 6.97 to 6.93 (m, 1H, C*H* of Dipp), 6.83 to 6.81 (m, 2H, C*H* of Dipp), 3.39 (sept, J = 6.9 Hz, 2H, C*H* of *i*Pr), 2.80 (sep, J = 6.8 Hz, 2H, C*H* of *i*Pr), 1.31 (d, J = 6.9 Hz, 6H, *Me* of *i*Pr), 1.09 (d, J = 6.8 Hz, 6H, *Me* of *i*Pr), 1.07 (d, J = 6.9 Hz, 12H, *Me* of *i*Pr), 0.27 (s, 18H, Si*Me*$_3$); **^{1}H{^{11}B} NMR** (C_6D_6): δ = 7.08 to 7.06 (m, 3H, C*H* of Dipp), 6.97 to 6.94 (m, 1H, C*H* of Dipp), 6.84 to 6.82 (m, 2H, C*H* of Dipp), 3.39 (sep, J = 6.9 Hz, 2H, C*H* of *i*Pr), 3.06 (s, 1H, B*H*), 2.99 (s, 1H, B*H*), 2.88 (s, 2H, B*H*), 2.79 (sep, J = 6.8 Hz, 2H, C*H* of *i*Pr), 2.77 (s, 2H, B*H*), 2.72 (s, 2H, B*H*), 2.21 (s, 2H, B*H*), 1.31 (d, J = 6.9 Hz, 6H, *Me* of *i*Pr), 1.10 (d, J = 6.7 Hz, 6H, *Me* of *i*Pr), 1.07 (d, J = 6.9 Hz, 12H, *Me* of *i*Pr), 0.27 (s, 18H, Si*Me*$_3$); **^{11}B NMR** (C_6D_6): δ = 36.6 (s, *B*N(SiMe$_3$)$_2$), 2.1 (d, J = 145.3 Hz, B_{Cb}), 0.6 (d, J = 146.7 Hz, B_{Cb}), −4.9 (d, J = 146.4 Hz, B_{Cb}), −9.8 (m, B_{Cb}); **^{11}B{^{1}H} NMR** (C_6D_6): δ = 36.4 (s, *B*N(SiMe$_3$)$_2$), 2.1 (s, B_{Cb}), −0.6 (s, B_{Cb}), −4.9 (s, B_{Cb}), −10.2 (s, B_{Cb}); **^{13}C{^{1}H} NMR** (C_6D_6): δ = 145.5 (*C* of Dipp), 144.0 (*C* of Dipp), 135.9 (*C* of Dipp), 129.9 (*C* of Dipp), 125.8 (*C* of Dipp), 123.6 (*C* of Dipp), 123.0 (*C* of Dipp), 89.7 (C of Cb), 30.0 (*C*HMe$_2$), 29.0 (*C*HMe$_2$), 25.2 (CH*Me*$_2$), 22.6 (*CHMe*$_2$), 21.1 (*CHMe*$_2$), 3.8 (Si*Me*$_3$); **HRMS (*m*/*z*)**: only **2b** was detected. **Elemental analysis**: calcd for $C_{34}H_{62}B_{11}N_3Si_2{\cdot}0.2C_5H_{12}$: C, 59.83; H, 9.22; N, 5.98; found C, 60.77; H, 8.92; N, 6.02.

3b′ was a brown oily residue that could not be purified, and no satisfactory NMR spectra were obtained. However, some diagnostic resonances were observed (see Fig. S46 and S47), and HRMS data support the proposed formulation. **^{1}H NMR** (C_6D_6): δ = 7.06 to 6.99 (m, 7H, C*H* of Dipp), 6.87 to 6.85 (m, 2H, C*H* of Dipp), 3.37 (sep, J = 7.2 Hz, 2H, C*H* of *i*Pr), 2.89 (sep, J = 6.9 Hz, 2H, C*H* of *i*Pr), 1.25 (d, J = 6.9 Hz, 6H, *Me* of *i*Pr), 1.10 (d, J = 6.9 Hz, 18H, *Me* of *i*Pr), 0.37 (s, 18H, Si*Me*$_3$); **^{11}B NMR** (C_6D_6): δ = 45.5 (s, *B*N(SiMe$_3$)$_2$), 2.1 to −0.2 (m, B_{Cb}), −5.2 (d, J = 154.3 Hz, B_{Cb}), −10.3 (br, B_{Cb}); **^{11}B{^{1}H} NMR** (C_6D_6): δ = 45.5 (s, *B*N(SiMe$_3$)$_2$), 1.6 (s, B_{Cb}), 0.1 (s, B_{Cb}), −5.1 (s, B_{Cb}), −10.3 (s, B_{Cb}); **HRMS (LIFDI)**: calcd for $C_{34}H_{62}B_{11}N_3Si_2$, 689.5506; found 689.5514.

Synthesis of 4

When the toluene solution **3** was stored at room temperature, it gradually converted to a brown oil **3′**, reaching full conversion within 8 days. Subsequent addition of 1 equivalent of RNC to the resulting solution afforded **4**. Alternatively, heating **3** at 80 °C for 4 h followed by the addition of one equivalent of RNC also led to the formation of **4**. The reaction mixture was allowed to stand at −30 °C for 12 h, after which the resulting crystals were collected from the mother liquor, washed with cold solvent, and dried to give analytically pure **4a** (orange block crystals, 74 mg, 66%) or **4b** (orange block crystals, 47 mg, 35%).

4a: **^{1}H NMR** (C_6D_6): δ = 6.78 to 6.66 (m, 7H, C*H* of Xyl), 6.50 (d, J = 7.6, 2H, C*H* of Xyl), 3.66 to 2.22 (m, 10H, B*H*), 2.09 (s, 6H, *Me* of Xyl), 2.01 (s, 6H, *Me* of Xyl), 1.75 (s, 6H, *Me* of Xyl), 0.36 (s, 18H, Si*Me*$_3$); **^{1}H{^{11}B} NMR** (C_6D_6): δ = 6.78 to 6.67 (m, 7H, C*H* of Xyl), 6.52 (d, J = 7.6, 2H, C*H* of Xyl), 3.11 (s, 1H, B*H*), 2.88 (s, 3H, B*H*), 2.81 (m, 2H, B*H*), 1.70 (s, 2H, B*H*), 2.29 (s, 2H, B*H*), 2.09 (s, 6H, *Me* of Xyl), 2.01 (s, 6H, *Me* of Xyl), 1.75 (s, 6H, *Me* of Xyl), 0.36 (s, 18H, Si*Me*$_3$); **^{11}B NMR** (C_6D_6): δ = 0.2 (br, B_{Cb}), −5.4 (d, J = 141.7 Hz, B_{Cb}), −10.5 (br, B_{Cb}); **^{11}B{^{1}H} NMR** (C_6D_6): δ = 0.0 (br, B_{Cb}), −5.4 (s, B_{Cb}), −10.2 (br, B_{Cb}); **^{13}C{^{1}H} NMR** (C_6D_6): δ = 150.9 (C of Xyl), 144.0 (C of Xyl), 135.4 (C of Xyl), 123.9 (C of Xyl), 122.9 (C of Xyl), 78.1 (C of Cb), 19.1 (*C*HMe$_2$), 18.2 (*C*HMe$_2$), 18.1 (*C*HMe$_2$), 5.0 (Si*Me*$_3$); **elemental analysis**: calcd for $C_{35}H_{55}N_4B_{11}Si_2$: C, 59.47; H, 7.84; N, 7.93; found C, 59.83; H, 8.07; N, 7.61.

4b: **^{1}H NMR** (C_6D_6): δ = 7.02 to 6.91 (m, 7H, C*H* of Dipp), 6.84 to 6.82 (m, 2H, C*H* of Dipp), 3.38 (sep, J = 7.0 Hz, 2H, C*H* of *i*Pr), 2.81 (sep, J = 6.8 Hz, 2H, C*H* of *i*Pr), 2.40 (br, 2H, C*H* of *i*Pr), 1.27 (d, J = 6.9 Hz, 6H, *Me* of *i*Pr), 1.24 (d, J = 6.8 Hz, 6H,

Me of *i*Pr), 1.06 (d, J = 6.9 Hz, 24H, *Me* of *i*Pr), 0.33 (s, 18H, Si*Me*$_3$); **^{1}H{^{11}B} NMR** (C_6D_6): δ = 7.03 to 6.91 (m, 7H, C*H* of Dipp), 6.84 to 6.82 (m, 2H, C*H* of Dipp), 3.38 (sep, J = 7.0 Hz, 2H, C*H* of *i*Pr), 3.09 (s, 1H, B*H*), 2.92 (s, 1H, B*H*), 2.86 (s, 2H, B*H*), 2.80 (sep, J = 6.8 Hz, 2H, C*H* of *i*Pr), 2.72 (br, 2H, C*H* of *i*Pr), 2.41 (s, 2H, B*H*), 2.26 (s, 2H, B*H*), 1.27 (d, J = 7.0 Hz, 6H, *Me* of *i*Pr), 1.24 (d, J = 6.9 Hz, 6H, *Me* of *i*Pr), 1.06 (d, J = 6.9 Hz, 24H, *Me* of *i*Pr), 0.33 (s, 18H, Si*Me*$_3$); **^{11}B NMR** (C_6D_6): δ = 2.4 to −0.5 (m, B_{Cb}), −5.1 (d, J = 161.2 Hz, B_{Cb}), −10.3 (br, B_{Cb}); **^{11}B {^{1}H} NMR** (C_6D_6): δ = 1.8 (s, B_{Cb}), 0.1 (s, B_{Cb}), −5.2 (s, B_{Cb}), −11.3 (s, B_{Cb}); **^{13}C{^{1}H} NMR** (C_6D_6): δ = 144.9 (*C* of Dipp), 141.7 (*C* of Dipp), 134.9 (*C* of Dipp), 125.4 (*C* of Dipp), 124.4 (*C* of Dipp), 123.1 (*C* of Dipp), 122.7 (*C* of Dipp), 122.4 (*C* of Dipp), 77.8 (C of Cb), 31.6 (*C*HMe$_2$), 29.7 (*C*HMe$_2$), 28.9 (*C*HMe$_2$), 28.7 (*C*HMe$_2$), 24.9 (CH*Me*$_2$), 24.4 (*CHMe*$_2$), 22.7 (*CHMe*$_2$), 22.2 (*CHMe*$_2$), 21.1 (*CHMe*$_2$), 4.1 (Si*Me*$_3$); **HRMS (LIFDI)**: calcd for $C_{47}H_{79}N_4B_{11}Si_2$, 876.6867; found 876.6906.

Conflicts of interest

There are no conflicts to declare.

Data availability

The data supporting this article have been included as part of the supplementary information (SI). Supplementary information: experimental details, X-ray crystallographic and characterisation data. See DOI: **https://doi.org/10.1039/d5qi02191j**.

CCDC 2497356–2497362 (**2a–2c**, **3a**, **3b**, **4a** and **4b**) contain the supplementary crystallographic data for this paper.[13a–g]

Acknowledgements

Q. Y. thanks Julius-Maximilians-Universität Würzburg (JMU) for financial support. We thank Christoph Mahler and Liselotte Michels for their help with performing high-resolution mass spectrometry (HRMS) and elemental analysis (EA), respectively. We are also grateful to Rüdiger Bertermann and Laura Wolz for their assistance with solid-state and VT-NMR measurements.

References

1 J. Wang and Q. Ye, Borirenes and Boriranes: Development and Perspectives, *Chem. – Eur. J.*, 2024, **30**, e202303695.

2 (*a*) S. E. Denmark, K. Nishide and A. M. Faucher, On the generation and configurational stability of (2S,3S)-1,2,3-triphenylborirane, *J. Am. Chem. Soc.*, 1991, **113**, 6675–6676; (*b*) Y. L. Rao, H. Amarne, S. B. Zhao, T. M. McCormick, S. Martić, Y. Sun, R. Y. Wang and S. Wang, Reversible Intramolecular C–C Bond Formation/Breaking and Color Switching Mediated by a N,C-Chelate in (2-ph-py)BMes2 and (5-BMes2-2-ph-py)BMes2, *J. Am. Chem. Soc.*, 2008, **130**, 12898–12900; (*c*) C. Baik, Z. M. Hudson, H. Amarne and S. Wang, Enhancing the Photochemical Stability of N, C-Chelate Boryl Compounds: C–C Bond Formation versus C–C Bond cis,trans-Isomerization, *J. Am. Chem. Soc.*, 2009, **131**, 14549–14559; (*d*) C. Baik, S. K. Murphy and S. Wang, Switching of a Single Boryl Center in π-Conjugated Photochromic Polyboryl Compounds and Its Impact on Fluorescence Quenching, *Angew. Chem., Int. Ed.*, 2010, **49**, 8224–8227; (*e*) H. Braunschweig, C. Claes, A. Damme, A. Deißenberger, R. D. Dewhurst, C. Hörl and T. Kramer, A facile and selective route to remarkably inert monocyclic NHC-stabilized boriranes, *Chem. Commun.*, 2015, **51**, 1627–1630; (*f*) T. R. McFadden, C. Fang, S. J. Geib, E. Merling, P. Liu and D. P. Curran, Synthesis of Boriranes by Double Hydroboration Reactions of N-Heterocyclic Carbene Boranes and Dimethyl Acetylenedicarboxylate, *J. Am. Chem. Soc.*, 2017, **139**, 1726–1729; (*g*) J. C. Walton, T. R. McFadden and D. P. Curran, Generation and Structure of Unique Boriranyl Radicals, *J. Am. Chem. Soc.*, 2017, **139**, 16514–16517; (*h*) W. Dai, S. J. Geib and D. P. Curran, Ring-Opening Reactions of NHC-Boriranes with In Situ Generated HCl: Synthesis of a New Class of NHC-Boralactones, *J. Am. Chem. Soc.*, 2019, **141**, 3623–3629.

3 (*a*) H. Zhang, J. Wang, W. Yang, L. Xiang, W. Sun, W. Ming, Y. Li, Z. Lin and Q. Ye, Solution-Phase Synthesis of a Base-Free Benzoborirene and a Three-Dimensional Inorganic Analogue, *J. Am. Chem. Soc.*, 2020, **142**, 17243–17249; (*b*) Y. Wei, J. Wang, W. Yang, Z. Lin and Q. Ye, Boosting Ring Strain and Lewis Acidity of Borirane: Synthesis, Reactivity and Density Functional Theory Studies of an Uncoordinated Arylborirane Fused to o-Carborane, *Chem. – Eur. J.*, 2022, **29**, e202203265; (*c*) L. Tan, J. Chen, X. Liu, A. Matler, N. Schopper, M. Finze, Z. Lin and Q. Ye, Antiaromatic 2-Azaboroles with π4σ2 Electronic Configuration, *J. Am. Chem. Soc.*, 2024, **146**, 31681–31690.

4 (*a*) C. Zhang, J. Wang, W. Su, Z. Lin and Q. Ye, Synthesis, Characterization, and Density Functional Theory Studies of Three-Dimensional Inorganic Analogues of 9,10-Diboraanthracene—A New Class of Lewis Superacids, *J. Am. Chem. Soc.*, 2021, **143**, 8552–8558; (*b*) C. Zhang, X. Liu, J. Wang and Q. Ye, A Three-Dimensional Inorganic Analogue of 9,10-Diazido-9,10-Diboraanthracene: A Lewis Superacidic Azido Borane with Reactivity and Stability, *Angew. Chem., Int. Ed.*, 2022, **61**, e202205506; (*c*) C. Zhang, J. Wang, Z. Lin and Q. Ye, Synthesis, Characterization, and Properties of Three-Dimensional Analogues of 9-Borafluorenes, *Inorg. Chem.*, 2022, **61**, 18275–18284; (*d*) M. O. Akram, J. R. Tidwell, J. L. Dutton and C. D. Martin, Tris(ortho-carboranyl)borane: An Isolable, Halogen-Free, Lewis Superacid, *Angew. Chem., Int. Ed.*, 2022, **61**, e202212073; (*e*) M. O. Akram, J. R. Tidwell, J. L. Dutton and C. D. Martin, Bis(1-Methyl-ortho-Carboranyl)Borane, *Angew. Chem., Int. Ed.*, 2023, **62**, e202307040; (*f*) L. Xiang, J. Wang, I. Krummenacher, K. Radacki, H. Braunschweig, Z. Lin and Q. Ye, Persistent and Predominantly Localized Boron Radical from the

Reduction of a Three-Dimensional Analogue of NHC-Stabilized Borafluorenium, *Chem. – Eur. J.*, 2023, **29**, e202301270; (*g*) S. Yruegas, J. C. Axtell, K. O. Kirlikovali, A. M. Spokoyny and C. D. Martin, Synthesis of 9-borafluorene analogues featuring a three-dimensional 1,1′-bis(o-carborane) backbone, *Chem. Commun.*, 2019, **55**, 2892–2895; (*h*) J. Krebs, A. Hafner, S. Fuchs, X. Guo, F. Rauch, A. Eichhorn, I. Krummenacher, A. Friedrich, L. Ji, M. Finze, Z. Lin, H. Braunschweig and T. B. Marder, Backbone-controlled LUMO energy induces intramolecular C–H activation in ortho-bis-9-borafluorene-substituted phenyl and o-carboranyl compounds leading to novel 9,10-diboraanthracene derivatives, *Chem. Sci.*, 2022, **13**, 14165–14178; (*i*) T. Bischof, X. Guo, I. Krummenacher, L. Beßler, Z. Lin, M. Finze and H. Braunschweig, Alkene insertion reactivity of a o-carboranyl-substituted 9-borafluorene, *Chem. Sci.*, 2022, **13**, 7492–7497; (*j*) V. I. Bregadze, *Chem. Rev.*, 1992, **92**, 209–223; (*k*) L. Xiang, J. Wang, A. Matler and Q. Ye, Structure-constraint induced increase in Lewis acidity of tris(ortho-carboranyl)borane and selective complexation with Bestmann ylides, *Chem. Sci.*, 2024, **15**, 17944–17949; (*l*) L. Xiang, A. Matler, L. Tan and Q. Ye, Reactivity study of Lewis superacidic carborane-based analogue of 9-bromo-9-borafluorene towards Lewis bases, *Dalton Trans.*, 2024, **53**, 11655–11658; (*m*) L. Xiang, A. G. Albacar, J. Wang, A. Matler, T. Preitschopf, M. Finze and Q. Ye, An Inorganic Version of Alkyne–Azide Cycloaddition: Click-Like Reactions of an o-Carboranyl Iminoborane with Organic Azides, *Organometallics*, 2025, **44**, 1756–1759; (*n*) J. Wang, L. Xiang, X. Liu, A. Matler, Z. Lin and Q. Ye, Avenue to novel o-carboranyl boron compounds–reactivity study of o-carborane-fused aminoborirane towards organic azides, *Chem. Sci.*, 2024, **15**, 4839–4845.

5 (*a*) H. Wang, J. Zhang and Z. Xie, Reversible Photothermal Isomerization of Carborane-Fused Azaborole to Borirane: Synthesis and Reactivity of Carbene-Stabilized Carborane-Fused Borirane, *Angew. Chem., Int. Ed.*, 2017, **56**, 9198–9201; (*b*) H. Wang, J. Zhang and Z. Xie, Ring-opening and ring-expansion reactions of carborane-fused borirane, *Chem. Sci.*, 2021, **12**, 13187–13192.

6 J. Wang, P. Jia, W. Sun, Y. Wei, Z. Lin and Q. Ye, Synthesis of Iminoboryl o-Carboranes by Lewis Base Promoted Aminoborirane-to-Iminoborane Isomerization, *Inorg. Chem.*, 2022, **61**, 8879–8886.

7 L. Xiang, J. Wang, N. Knoblauch, A. Matler and Q. Ye, Conversion of Bestmann Ylide into Carbophosphinocarbene, *Angew. Chem., Int. Ed.*, 2025, **64**, e202501955.

8 (*a*) F. Sun, S. Tan, H.-J. Cao, C.-S. Lu, D. Tu, J. Poater, M. Solà and H. Yan, Facile Construction of New Hybrid Conjugation via Boron Cage Extension, *J. Am. Chem. Soc.*, 2023, **145**, 3577–3587; (*b*) Z. Sun, J. Zong, H. Ren, C. Lu, D. Tu, J. Poater, M. Solà, Z. Shi and H. Yan, Couple-close construction of non-classical boron cluster-phosphonium conjugates, *Nat. Commun.*, 2024, **15**, 7934; (*c*) Z. Wang, X. Gou, Q. Shi, K. Liu, X. Chang, G. Wang, W. Xu, S. Lin, T. Liu and Y. Fang, Through-Space Charge Transfer: A New Way to Develop a High-Performance Fluorescence Sensing Film towards Opto-Electronically Inert Alkanes, *Angew. Chem., Int. Ed.*, 2022, **61**, e202207619; (*d*) K. R. Wee, Y. J. Cho, S. Jeong, S. Kwon, J. D. Lee, I. H. Suh and S. O. Kang, Carborane-based optoelectronically active organic molecules: wide band gap host materials for blue phosphorescence, *J. Am. Chem. Soc.*, 2012, **134**, 17982–17990; (*e*) J. J. Schwartz, A. M. Mendoza, N. Wattanatorn, Y. Zhao, V. T. Nguyen, A. M. Spokoyny, C. A. Mirkin, T. Baše and P. S. Weiss, Surface dipole control of liquid crystal alignment, *J. Am. Chem. Soc.*, 2016, **138**, 5957–5967; (*f*) P. Cui, X. Liu and G. Jin, Supramolecular architectures bearing half-sandwich iridium-or rhodium-based carboranes: Design, synthesis, and applications, *J. Am. Chem. Soc.*, 2023, **145**, 19440–19457; (*g*) Z. Lu, P. Qiu, H. Zhai, G. G. Zhang, X. W. Chen, Z. Lu, Y. Wu and X. Chen, Facile Synthesis of Potassium Decahydrido-Monocarba-closo-Decaborate Imidazole Complex Electrolyte for All-Solid-StatePotassium Metal Batteries, *Angew. Chem., Int. Ed.*, 2024, **63**, e202412401; (*h*) M. Scholz and E. Hey-Hawkins, Carbaboranes as pharmacophores: properties, synthesis, and application strategies, *Chem. Rev.*, 2011, **111**, 7035–7062; (*i*) P. Stockmann, M. Gozzi, R. Kuhnert, M. B. Sárosi and E. Hey-Hawkins, New keys for old locks: Carborane-containing drugs as platforms for mechanism-based therapies, *Chem. Soc. Rev.*, 2019, **48**, 3497–3512.

9 (*a*) G. Qiu, Q. Ding and J. Wu, Recent advances in isocyanide insertion chemistry, *Chem. Soc. Rev.*, 2013, **42**, 5257–5269; (*b*) A. Dömling, Recent Developments in Isocyanide Based Multicomponent Reactions in Applied Chemistry, *Chem. Rev.*, 2006, **106**, 17–89; (*c*) A. Dömling and I. Ugi, Multicomponent Reactions with Isocyanides, *Angew. Chem., Int. Ed.*, 2000, **39**, 3168–3210.

10 (*a*) H. Braunschweig, M. A. Celik, R. D. Dewhurst, K. Ferkinghoff, A. Hermann, J. O. Jimenez-Halla, T. Kramer, K. Radacki, R. Shang and E. Siedler, Interactions of Isonitriles with Metal–Boron Bonds: Insertions, Coupling, Ring Formation, and Liberation of Monovalent Boron, *Chem. – Eur. J.*, 2016, **22**, 11736–11744; (*b*) H. Asakawa, K. H. Lee, Z. Lin and M. Yamashita, Facile scission of isonitrile carbon–nitrogen triple bond using a diborane(4) reagent, *Nat. Commun.*, 2014, **5**, 4245; (*c*) M. Suginome, T. Fukuda, H. Nakamura and Y. Ito, Synthesis of (Boryl)(silyl)iminomethanes by Insertion of Isonitriles into Silicon–Boron Bonds, *Organometallics*, 2000, **19**, 719–721.

11 (*a*) H. Braunschweig, R. D. Dewhurst, F. Hupp, M. Nutz, K. Radacki, C. W. Tate, A. Vargas and Q. Ye, Multiple complexation of CO and related ligands to a main-group element, *Nature*, 2015, **522**, 327–330; (*b*) M. Arrowsmith, D. Auerhammer, R. Bertermann, H. Braunschweig and M. A. Celik, From Borane to Borylene without Reduction: Ambiphilic Behavior of a Monovalent Silylisonitrile Boron Species, *Angew. Chem., Int. Ed.*, 2017, **56**, 11263–11267; (*c*) H. Braunschweig, R. D. Dewhurst, L. Pentecost,

K. Radacki, A. Vargas and Q. Ye, Dative Bonding between Group 13 Elements Using a Boron-Centered Lewis Base, *Angew. Chem., Int. Ed.*, 2016, **55**, 436–440.

12 (*a*) X. Liu, M. Heinz, J. Wang, L. Tan, M. C. Holthausen and Q. Ye, A Journey from Benzoborirene to Benzoborole-Supported 1,2-Diimine and Antiaromatic Boroledиide, *Angew. Chem., Int. Ed.*, 2023, **62**, e202312608; (*b*) M. Sindlinger, M. Ströbele, J. Grunenberg and H. F. Bettinger, Accessing unusual heterocycles: ring expansion of benzoborirenes by formal cycloaddition reactions, *Chem. Sci.*, 2023, **14**, 10478–10487; (*c*) M. Sindlinger, M. Strobele, C. Maichle-Mossmer and H. F. Bettinger, Kinetic stabilization allows structural analysis of a benzoborirene, *Chem. Commun.*, 2022, **58**, 2818–2821.

13 (*a*) CCDC 2497356: Experimental Crystal Structure Determination, 2025, DOI: **10.5517/ccdc.csd.cc2ptpw3**; (*b*) CCDC 2497357: Experimental Crystal Structure Determination, 2025, DOI: **10.5517/ccdc.csd.cc2ptpx4**; (*c*) CCDC 2497358: Experimental Crystal Structure Determination, 2025, DOI: **10.5517/ccdc.csd.cc2ptpy5**; (*d*) CCDC 2497359: Experimental Crystal Structure Determination, 2025, DOI: **10.5517/ccdc.csd.cc2ptpz6**; (*e*) CCDC 2497360: Experimental Crystal Structure Determination, 2025, DOI: **10.5517/ccdc.csd.cc2ptq08**; (*f*) CCDC 2497361: Experimental Crystal Structure Determination, 2025, DOI: **10.5517/ccdc.csd.cc2ptq19**; (*g*) CCDC 2497362: Experimental Crystal Structure Determination, 2025, DOI: **10.5517/ccdc.csd.cc2ptq2b**.